Advanced Template Matching Algorithm for Instantaneous Heartbeat Detection using Continuous Wave Radar Systems

Christoph Will, Kilin Shi, Robert Weigel, and Alexander Koelpin
Institute for Electronics Engineering, Friedrich-Alexander University of Erlangen-Nuremberg
Cauerstr. 9, 91058 Erlangen, Germany
Phone: +49(0)9131 85-27190, Email: christoph.will@fau.de

***Abstract*—Instantaneous heartbeat detection is a key parameter in modern vital sign monitoring. Continuous wave (CW) radar systems enable contactless measurements of the vibrations on the human skin effected by heartbeats. Since a high accuracy as well as robustness of the measurement sensor is appreciated, the belonging signal processing routine has to deal with challenging requirements. In this paper, an advanced template matching (ATM) algorithm is proposed to enhance the performance regarding instantaneous heartbeat detection using CW radar systems. Compared to common template matching algorithms, multiple heterogeneous templates are utilized in this approach, at which the appropriate template type is determined by prior feature detection. A 24 Ghz Six-Port microwave interferometer is used for vital sign measurements of a person-under-test. The functionality of the proposed algorithm is verified by a synchronous reference electrocardiogram (ECG) and its enhancement is shown by reducing the root-mean-square error (RMSE) of the interbeat intervals (IBI) compared to an ordinary template matching algorithm.**

***Index Terms*—biomedical signal processing, digital signal processing, electromagnetic measurements, radar interferometry, radar signal processing.**

I. Introduction

Accurate vital sign monitoring is essential in hospitals, but additionally, it is useful if not even required in further application fields. Health status recognition of a car driver [1] and monitoring of a sleeping child at home to expeditiously detect apnea or the Sudden Infant Death Syndrome [2] are just two examples. Since contactless measurements of breathing and heartbeat are appreciated in such application examples, radar based approaches are preferred to electrocardiography (ECG), ballistocardiography (BCG) or photoplethysmography (PPG). Radar systems utilize the large difference of the electromagnetic permitivity between air and human skin which causes a reflection of the emitted radio frequency (RF) signal. Heartbeats cause vibrations on the thorax which can be detected as Doppler shifts by CW radar systems.

First radar based vital sign detection was achieved in 1975, at which the respiration of a cat was monitored [3]. Over the years the radar technique advanced and the research on CW radar systems for vital sign monitoring increased in the early 90s [4]. Beside hardware enhancements, the corresponding signal processing routines were improved, too. Previously published algorithms mostly determine the heart rate of the person-under-test. In [5], for instance, the periodicity of the heartbeat is utilized within an autocorrelation based approach.

If heart rate identification is not sufficient and instantaneous heartbeat detection is required, advanced algorithms have to be used. A cross-correlation based template matching for CW radar systems was published in [6]. Similar to BCG [7] and PPG [8] based template matching approaches, the signal curve of the used templates included the dicrotic notch which depicts a typical characteristic in pulse signals [9]. The closing of the cardiac valve as well as reflections of the vasodile blood wave at blood vessels and forks cause this notch. In some cases a second notch caused by the venous pulse effect produces another local maximum prior to the main maximum of a heartbeat signal [9]. Especially on the thorax several effects are superimposed [10], for which reason the heartbeat signal curve can have different shapes. Additionally, the required filtering to extract the heartbeat signal has an influence on the resulting signal curve. Therefore, using a single template is insufficient for a desired perfect detection probability.

Several algorithms have been published to enhance the robustness of radar based vital sign monitoring, like random body movement cancelation [11]. In this paper, a different approach for an increased robustness is proposed, the usage of multiple heterogeneous templates. These templates are defined by various features, similar to a feature based correlation algorithm for ultra-wideband (UWB) radar systems [12]. Prior to the measurements, a training phase is necessary, in which several templates of each type are generated. During subsequent classification these templates are utilized for a fast and accurate heartbeat detection.

II. Advanced Template Matching

A. Defininig the heterogeneous template types

Since a single heartbeat signal shape as template type implicates limited robustness regarding different persons-under-test and varying measurement points on the body, the proposed ATM algorithm utilizes a variety of templates which can be categorized in five heterogeneous types. Exemplary curves of the unequal heartbeat signal shapes are shown in Fig. 1. Type 2 depicts the signal shape of the templates used in [6], including the dicrotic notch. The other types were defined due to their similarly high occurrence probability in empirical investigations of heartbeat signal shapes of different persons-under-test.

The signal shape of every template type contains multiple characteristic points, which are declared as features. These

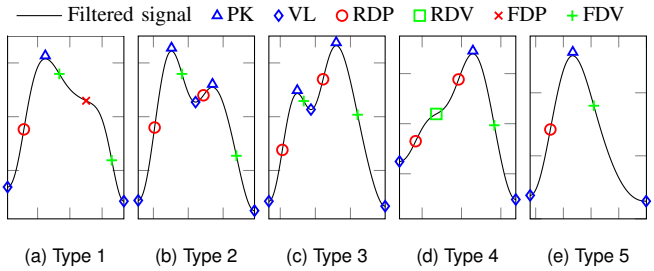

Fig. 1. Five heterogeneous types of heartbeat curves.

are the six features that are also used in the feature based correlation approach for UWB radar systems published in [12]:

- PK: peak ($dx(t)/dt = 0$ and $d^2x(t)/dt^2 < 0$)
- VL: valley ($ds(t)/dt = 0$ and $d^2s(t)/dt^2 > 0$)
- RDP: rising derivative peak ($ds(t)/dt > 0$, $d^2s(t)/dt^2 = 0$ and $d^3s(t)/dt^3 < 0$)
- RDV: rising derivative valley ($ds(t)/dt > 0$, $d^2s(t)/dt^2 = 0$ and $d^3s(t)/dt^3 > 0$)
- FDP: falling derivative peak ($ds(t)/dt < 0$, $d^2s(t)/dt^2 = 0$ and $d^3s(t)/dt^3 < 0$)
- FDV: falling derivative valley ($ds(t)/dt < 0$, $d^2s(t)/dt^2 = 0$ and $d^3s(t)/dt^3 > 0$)

The sequences of the feature occurrences are specific for the signal shapes of every template type, whereas the start as well as the end of all template types are each defined by valleys:

(1) VL→RDP→PK→FDV→FDP→FDV→VL
(2) VL→RDP→PK→FDV→VL→RDP→PK→FDV→VL
(3) VL→RDP→PK→FDV→VL→RDP→PK→FDV→VL
(4) VL→RDP→RDV→RDP→PK→FDV→VL
(5) VL→RDP→PK→FDV→VL

B. Challenges of the feature detection

Since type 2 and type 3 have the same feature sequence, the heights of the two peaks within one signal curve have to be compared amongst each other. If the first peak is higher than the second one, the investigated signal cutout is a type 2 heartbeat shape. Otherwise, the signal output depicts a type 3 shape with the dicrotic notch prior to the main heartbeat peak.

A second inconvenience represents the fact that two consecutive type 5 heartbeats have the same feature sequence as one type 2 and type 3 heartbeat shape. Therefore, to distinguish two consecutive type 5 heartbeats from the other two cases, additional curve characteristics have to be examined. Here, the time difference between the two peaks compared to the latest detected interbeat interval (IBI) values is a criteria as well as the prominence ("height") of the valley between the two peaks regarding the ordinate values of the outer valleys. The curve cutout is determined as a type 2 or type 3 heartbeat shape if the valley in the mid is positioned higher than the half of the maximal height of whole cutout and simultaneously higher than both outer valleys.

C. Training stage

Before ATM based heartbeat detection measurements are possible, a template database has to be generated within a *training stage*. Here, the heartbeat signals of one or better various persons are measured by the used radar system for a sufficient time frame to ensure that multiple signal curves for every heartbeat type are acquired. Contemporaneously, during training, an ECG signal of the particular person-under-test has to be synchronously recorded to enable a subsequent verification of the determined heartbeat positions.

The acquired radar signal is filtered and subsequently investigated regarding the template types 1...4 by scanning the signal for their specific feature sequence. No templates are generated for the type 5 heartbeat shape since the peak prominence as well as the time difference to the adjacent peaks are examined. The correctness of the heartbeat detection for the signal shape types 1...4 are verified by means of the ECG reference. For correct detections, the corresponding cutout, whose borders are defined by the (outer) valleys, is extracted and saved as an exemplary template for its appropriate type. Additionally, the cutout is resampled to a predefined normalized sample length m to ensure a proper comparability independent of the sample rate during classification.

D. Classification stage

The first step during classification of new measurement data is extracting the previously defined features. The extracted features are afterward used to detect the sequence types 1...4 within the measured signal just as during the training stage. When a characteristic sequence is detected, the appropriate cutout is resampled to the normalized sample length m. Thereafter, this cutout A_m is cross-correlated with all saved templates $B_{m,i}$ of the corresponding type, which were generated within the training stage, to calculate the correlation coefficients r_i, at which the zero-mean values of both vectors are used:

$$r_i = \frac{\sum_m \left(A_m - \bar{A}\right) \cdot \left(B_{m,i} - \bar{B}_i\right)}{\sqrt{\sum_m \left(A_m - \bar{A}\right)^2 \cdot \sum_m \left(B_{m,i} - \bar{B}_i\right)^2}} \tag{1}$$

If one correlation coefficient is higher than a predefined threshold r_{min}, the examined cutout is determined as a heartbeat. The exact position of the occurred heartbeat is defined by the (higher) peak within the cutout. For type 2 or type 3 curve shapes, the lower peak is explicitly marked as a non-heartbeat. The remaining type 5 peaks are classified regarding their prominence and their distances to the adjacent peaks.

III. Measurement System

New vital sign measurements were performed to verify the functionality of the proposed algorithm. Here, a Six-Port microwave interferometer was used, which is a specific type of CW radar. Primarily invented for power measurements by Engen and Hoer in the 1970s [13], the Six-Port network is nowadays also utilized as a quadrature interferometer [14] for

radar applications. The complete passive structure implicates a high phase accuracy as well as a low power consumption and low costs. In these measurements, a monostatic system variant was chosen, whose block diagram is depicted in Fig. 2. The radio frequency (RF) signal is generated by a *PSG Analog Signal Generator E8257D* from *Keysight* at a frequency of 24,05 GHz and an output power of 5 dBm. A 10 dB coupler splits this RF signal into two parts, whereupon the major part is transmitted through a circulator to be emitted by a small horn antenna with a gain of 15 dB. The transmitting (TX) antenna is focused on the thorax of a person-under-test and simultaneously works as a receiving (RX) antenna. The received signal is fed through the circulator to one of the two Six-Port inputs. The other input port is fed by the minor output signal of the coupler.

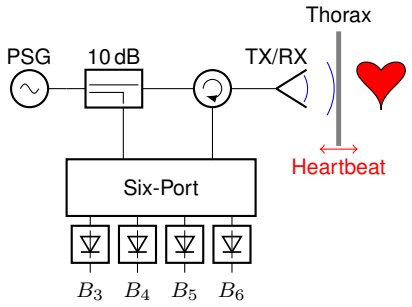

Fig. 2. Block diagram of the Six-Port sensor.

The two Six-Port input signals are superimposed within the network with relative phase shifts of multiples of $\pi/2$ between them which leads to four output signals. These are down-converted to the baseband voltages $B_{3...6}$ by four Schottky diode based envelope detectors *ADL6010* from *Analog Devices*. The four output voltages are sampled by analog-to-digital converters (ADC) and can be utilized to calculate the relative phase shift $\Delta\sigma$ between both input signals:

$$\Delta\sigma = \arg\{(B_5 - B_6) + j(B_3 - B_4)\}. \tag{2}$$

Since the vibration on the thorax due to heartbeats produce a phase shift of the reflected signal, relative displacements Δx can be calculated using the known wavelength λ:

$$\Delta x = \frac{\Delta\sigma}{2\pi} \cdot \frac{\lambda}{2}. \tag{3}$$

In this measurement system, the *ADS1298* from *Texas Instruments* with a resolution of 24 bit and a sample rate of 500 samples per second is used for data acquisition. The Six-Port baseband voltages are sampled differentially and synchronously with the output voltages of two electrodes that have to be attached on the person-under-test during the training stage. The acquired data is sent via Ethernet to a personal computer where further signal processing is performed.

IV. Measurement Results

During the performed measurements, the person-under-test was sitting at a distance of approximately half a meter to the antenna and was breathing normally. The *Lead II* of Einthoven's triangle, which is the voltage difference between a left leg electrode and right arm electrode [10], was chosen as ECG reference signal in the training stage and also for verification in the classification stage. The Pan-Tompkins algorithm [15] was utilized to detect the QRS complexes within the ECG signal. The values for the tuning parameters of the ATM algorithm were chosen as in the following:

- $f_l = 0.5$ Hz (lower bandpass cutoff frequency)
- $f_u = 3.0$ Hz (upper bandpass cutoff frequency)
- $r_{min} = 0.85$
- $d_{min} = 0.50$ (min. required distance to adjecent peaks)
- $p_{min} = 0.05$ (min. required prominence of the peak)

Here, the used bandpass filter was implemented as a forth order Butterworth filter, and d_{min} as well as p_{min} are the threshold values for a type 5 shape heartbeat classification. To emphasize the robustness of the algorithm, the person-under-test during this classification was another person than the one who was utilized in the training stage to generate the heartbeat templates. In total, around ten exemplary signal curves per template type were generated in the training stage. A classification cutout of the filtered radar signal as well as the detected features are illustrated in Fig. 3.

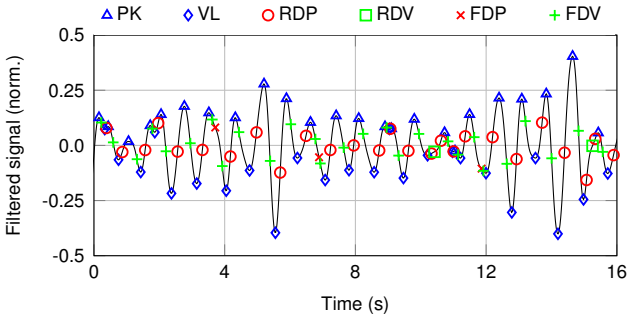

Fig. 3. Detected features in the filtered radar signal.

The corresponding heartbeat types determined by the ATM algorithm are shown in Fig. 4. The green crosses and diamonds as well as the blue squares depict peaks which were explicitly marked as non-heartbeats by the proposed algorithm.

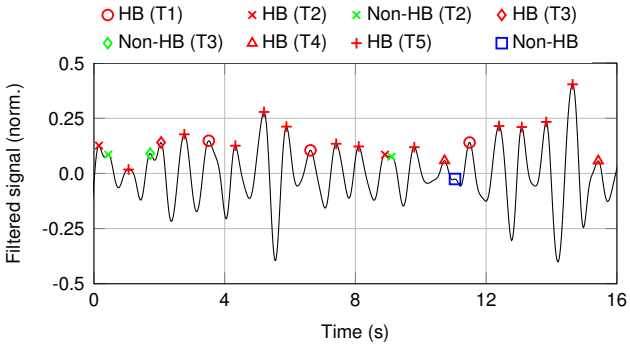

Fig. 4. Detected heartbeat types in the filtered radar signal.

The exact positions of the detected heartbeats in the belonging unfiltered radar signal are depicted in Fig. 5a, together with the detected R-peaks of the ECG reference signal. In subplot 5b the template matching results of the algorithm in [6] (XCF) are shown which enables a first accuracy comparison.

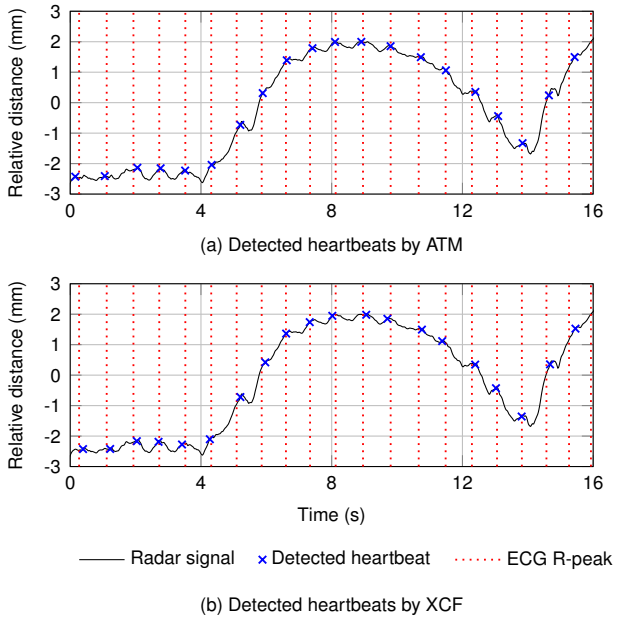

Fig. 5. Comparison of the detected heartbeats between ATM and XCF.

The resulting interbeat interval (IBI) curves are illustrated in Fig. 6 for an enlarged classification cutout. The IBI curves of both template matching algorithms are compared to the IBI of the reference ECG. The boundaries of ± 0.1 s around the reference IBI further emphasize the improvement of the ATM algorithm regarding accuracy and up-to-dateness. The RMSE could significantly be decreased from 68.2 ms to 18.0 ms.

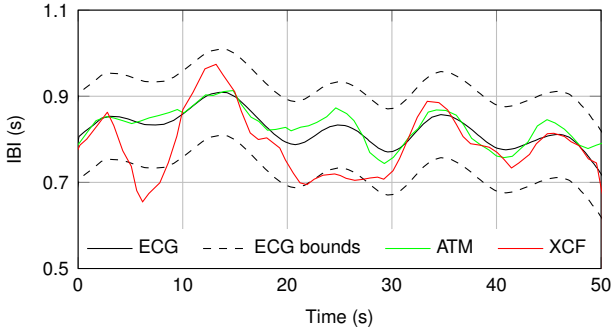

Fig. 6. Comparison of the IBI curves of ECG, ATM and XCF.

V. Conclusion

In this paper, an advanced template matching algorithm for an instantaneous heartbeat detection using CW radar systems was presented. The enhancement of the proposed algorithm, compared to previous template matching approaches, is a feature detection prior to the cross-correlation and the utilization of multiple templates of heterogeneous template types which improves the robustness as well as the accuracy of the heartbeat detection. A Six-Port microwave interferometer and a reference ECG were used for verification measurements. Despite the fact that the used templates had been generated with a different person within a prior training stage, the resulting RMSE could significantly be decreased compared to the previous template matching algorithm.

References

[1] G. Vinci, T. Lenhard, C. Will, and A. Koelpin, "Microwave interferometer radar-based vital sign detection for driver monitoring syst," in *2015 IEEE MTT-S International Conference on Microwaves for Intelligent Mobility (ICMIM)*, April 2015, pp. 1–4.

[2] P. Peirano, B. Signh, J. Lacombe, H. Cherrier, and N. Monod, "Cardiorespiratory patterns during sleep and wakefulness in infants who subsequently died of SIDS," in *Engineering in Medicine and Biology Society, 1988. Proceedings of the Annual International Conference of the IEEE*, Nov 1988, pp. 1930–1931 vol.4.

[3] J. C. Lin, "Noninvasive microwave measurement of respiration," *Proceedings of the IEEE*, vol. 63, no. 10, pp. 1530–1530, Oct 1975.

[4] ——, "Microwave sensing of physiological movement and volume change: A review," *Bioelectromagnetics*, vol. 13, no. 6, pp. 557–565, 1992.

[5] C. Will, K. Shi, F. Lurz, R. Weigel, and A. Koelpin, "Intelligent signal processing routine for instantaneous heart rate detection using a Six-Port microwave interferometer," in *2015 International Symposium on Intelligent Signal Processing and Communication Systems (ISPACS)*, Nov 2015, pp. 483–487.

[6] ——, "Instantaneous heartbeat detection using a cross-correlation based template matching for continuous wave radar systems," in *2016 IEEE Topical Conference on Wireless Sensors and Sensor Networks (WiSNet)*, Jan 2016, pp. 31–34.

[7] J. Shin, B. Choi, Y. Lim, D. Jeong, and K. Park, "Automatic ballistocardiogram (BCG) beat detection using a template matching approach," in *Engineering in Medicine and Biology Society, 2008. EMBS 2008. 30th Annual International Conference of the IEEE*, Aug 2008, pp. 1144–1146.

[8] P. Prakash, M. Sareen, R. Anand, Abhinav, and S. Anand, "Application of wavelets based multiresolution analysis to detect relevant points of interest from finger-tip photoplethesmography and pressure signal from the radial artery," in *Biomedical Engineering Conference, 2008. CIBEC 2008. Cairo International*, Dec 2008, pp. 1–4.

[9] K. Shelley and S. Shelley, "Pulse oximeter waveform: photoelectric plethysmography," *Clinical Monitoring, Carol Lake, R. Hines, and C. Blitt, Eds.: WB Saunders Company*, pp. 420–428, 2001.

[10] S. Silbernagl, *Taschenatlas der Physiologie*. Georg Thieme Verlag, 2007.

[11] C. Li and J. Lin, "Complex signal demodulation and random body movement cancellation techniques for non-contact vital sign detection," in *Microwave Symposium Digest, 2008 IEEE MTT-S International*, June 2008, pp. 567–570.

[12] T. Sakamoto, R. Imasaka, H. Taki, T. Sato, M. Yoshioka, K. Inoue, T. Fukuda, and H. Sakai, "Feature-based correlation and topological similarity for interbeat interval estimation using ultrawideband radar," *IEEE Transactions on Biomedical Engineering*, vol. 63, no. 4, pp. 747–757, April 2016.

[13] G. F. Engen and C. A. Hoer, "Application of an arbitrary 6-port junction to power-measurement problems," *Instrumentation and Measurement, IEEE Transactions on*, vol. 21, no. 4, pp. 470–474, Nov 1972.

[14] A. Koelpin, F. Lurz, S. Linz, S. Mann, C. Will, and S. Lindner, "Six-port based interferometry for precise radar and sensing applications," *Sensors*, vol. 16, no. 10, p. 1556, 2016. [Online]. Available: http://www.mdpi.com/1424-8220/16/10/1556

[15] J. Pan and W. J. Tompkins, "A real-time QRS detection algorithm," *Biomedical Engineering, IEEE Transactions on*, vol. BME-32, no. 3, pp. 230–236, March 1985.